Supplementary Information

Leukocyte-Inspired Multiscale Hierarchical Interface for High-Efficiency Capture and Gentle Release of Circulating Tumor Cells

Yujie, Lv[a,#], Jin Yang[a,#], Ronghua Wang[a], Jianwen Hou[b], Xinhao Peng[c,], Xia Liu[a,]*, Shuxun Cui[d,]**

[a] School of Chemistry, Southwest Jiaotong University, Chengdu, 610031, China

[b] Institute of Biomedical Engineering, College of Medicine, Southwest Jiaotong University, Chengdu, 610031, China

[c] Department of Oncology, Affiliated Hospital of Southwest Jiaotong University, The Third People's Hospital of Chengdu, Chengdu, 610031, China

[d] Department of Chemistry, College of Sciences, Northeastern University, Shenyang, 110819, China

Additional Experimental Section

Additional Scheme S1

Additional Figures S1-S11

Additional Tables S1-S3

Additional References

1. Additional Experimental Section

1.1 Synthesis of tetra-ortho-methoxy-substituted azobenzene (mAzo)

mAzo was successfully synthesized according to the literature.[1] Briefly, as in Figure S3a, 2,6-dimethoxyaniline (1.54 g, 10 mmol) was dissolved in dilute hydrochloric acid (4.32 mL, 21%) and cooled to 0 - 5℃ in an ice bath. $NaNO_2$ (0.69 g, 10 mmol) dissolved in 6.67 mL of H_2O was slowly added to the above solution and stirred for 20 min with the temperature always maintained at 0 - 5℃. The above diazonium salt was then slowly added to a 20 mL suspension of an ice-water mixture mixed with 3, 5-dimethoxyaniline (1.54 g, 10 mmol), and the pH of the mixture was adjusted to 8 - 9 with saturated sodium bicarbonate solution and stirred overnight. Finally, the red crude product was filtered and purified by chromatography using methanol/ethyl acetate (1:4) as eluent to obtain the final product mAzo.

1.2 Preparation of SoS silica microspheres

SoS silica microspheres were synthesized with minor modifications based on previously reported methods.[2] First, PVA (0.25 g) was dissolved in water (5 mL) by ultrasonication, while CTAB (0.10 g) was added later under magnetic stirring. Then methanol (8 mL) and ammonium hydroxide (2 mL, 1.4%) were sequentially added to the above solution. After magnetic stirring for 15 min, CPTMS (500 μL) was added drop by drop, and then stirred at room temperature for 24 h. The white solid product was collected by centrifugation at 11,000 rpm and washed with ethanol, and then dried in a vacuum to obtain SoS silica microspheres.

1.3 Calculation of specific surface area of SoS silica microsphere

D and d were used to represent the particle sizes of large and small spheres in SoS silica microspheres, respectively. In the case of the large particle size ratio of the large sphere to the small sphere, the effect of the curved surface of the large sphere on the spatial alignment of small spheres was neglected. In the case of aligned small spheres, the number of small spheres (Q_{small}) was calculated from the ratio of the surface area of the large sphere (S_{large}) to the cross-sectional area of the small spherical hemisphere (A):

$$Q_{small} = \frac{S_{large}}{A} = \frac{4\pi\left(\frac{D}{2}\right)^2}{\pi\left(\frac{d}{2}\right)^2} \quad \text{(S1)}$$

The specific surface area of SoS silica microsphere ($S_{V(SoS)}$) was calculated from the ratio of the surface area of all the small spherical hemispheres (S_{small}) to the volume of the whole SoS silica microsphere (V_{SoS}):

$$S_{V(SoS)} = \frac{S_{small}}{V_{SoS}} = \frac{\frac{4\pi\left(\frac{d}{2}\right)^2}{2}Q_{small}}{\frac{4}{3}\pi\left(\frac{D}{2}\right)^3 + \frac{\frac{4}{3}\pi\left(\frac{d}{2}\right)^3}{2}Q_{small}} \quad \text{(S2)}$$

The specific surface area of smooth silica microsphere ($S_{V(large)}$) was calculated by the ratio of the surface area of the large sphere (S_{large}) to its volume (V_{large}):

$$S_{V(large)} = \frac{S_{large}}{V_{large}} = \frac{4\pi\left(\frac{D}{2}\right)^2}{\frac{4}{3}\pi\left(\frac{D}{2}\right)^3} \quad \text{(S3)}$$

Based on the aforementioned calculations, it can be inferred that the specific surface area of the SoS silica microspheres is approximately twice that of the smooth silica microspheres.

1.4 Cell culture and blood samples processing

In our experiments, MCF-7, HeLa and HepG2 cells were selected as model target cells, and all were cultured at 37℃ in a 5% CO_2 environment, with HepG2 using minimum essential medium (MEM) (supplemented with 10% FBS and 1% antibiotics), and the other cells were cultured in Dulbecco's modified Eagle's medium (DMEM) (supplemented with 10% FBS and 1% antibiotics). Human whole blood samples were provided by the Third People's Hospital of Sichuan Province (blood collection was performed according to the guidelines issued by the Ethics Committee of the Academy of Medical Sciences and the Third People's Hospital of Sichuan Province). Whole blood samples were then treated with ACK lysis buffer according to the instructions of the manufacturer.

1.5 Cytocompatibility testing

Cell viability was comprehensively evaluated by Calcein-AM/PI staining method and CCK-8 assay. Three different types of cancer cells were inoculated into 24-well plates at a density of 1×10^5 cells per mL and incubated until their complete adherence and spreading, and then co-incubated with different substrates. After 24 h, the samples were stained with Calcein-AM and PI. Cells staining positively for Calcein-AM or PI were considered as alive or dead, respectively. The procedure described for the co-incubation of cells with the material was repeated. After 24 h, the samples were assayed according to the instructions for use of the CCK-8 kit, and the absorbance of the solution at 450 nm was measured by a microplate reader.

1.6 Cancer cell capture assay

In order to validate the effect of g@SoS-PACF nanosubstrate on the capture of cancer cells, we investigated the capture efficiency of g@SoS, g@SoS-P, and g@SoS-PACF nanosubstrates

toward cancer cells, as well as the affinity toward cells of the two-dimensional cell capture interface of g-NH_2-FA and the three-dimensional nanosubstrate of g@SoS-PACF. The effect of incubation time of cell capture on capture efficiency was explored by incubating 1×10^5 HeLa cells with g@SoS, g@SoS-P, and g@SoS-PACF nanosubstrates in a shaker for different times (5 - 120 min) at 37℃, aspirating the supernatant and gently rinsing three times with PBS to remove uncaptured cells, and counting them by a cell counter. The capture efficiency was calculated according to the following formula:

$$\text{Capture efficiency} = \frac{Total\ number\ of\ cells\ added - Number\ of\ uncaptured\ cells}{Total\ number\ of\ cells\ added} \times 100\% \quad \text{(S4)}$$

Finally, g@SoS-PACF nanosubstrate was incubated with EpCAM-positive cells (MCF-7, HepG2) for 60 min to demonstrate its broad-spectrum capture performance.

1.7 Determination of binding constants for various substrates in interaction with cancer cells

To evaluate the binding performance of g-NH_2-FA and g@SoS-PACF toward target cells, HeLa cells were pre-stained with DAPI. The cells were incubated with g-NH_2-FA and g@SoS-PACF substrates immobilized with varying concentrations of FA following the capture protocol described above, followed by three washes with PBS. The fluorescence intensity of pre-stained HeLa cells in the supernatant was measured using a microplate reader, $\lambda_{ex}/\lambda_{em}$= 360 nm/460 nm. The fluorescence from the captured cells was estimated by subtraction. The fluorescence intensity (Y) was normalized and fitted to the folate concentration (X) to obtain K_d values according to the following equation:

$$Y = B_{max}X/(K_d+X) \quad \text{(S5)}$$

1.8 Rare-cell capture performance of the g@SoS-PACF substrate

To study the capture of rare cells, synthetic samples were prepared by adding different numbers of HeLa cells (10 - 300 cells) into 1 mL of PBS. Similarly, artificial samples were prepared by admixing different numbers of HeLa cells (10 - 300 cells) into 1 mL of treated healthy blood. The rare-cell capture performance of the g@SoS-PACF substrate was evaluated following the capture procedure described above.

1.9 Release of captured cells and analysis of cell viability

The captured cells were irradiated under LED red light source (620 nm) system for different times (5 - 30 min), the supernatant was aspirated and gently moistened three times with PBS, and the number of released cells was counted with a cell counter. Release efficiency $= \frac{Number\ of\ released\ cells\ in\ the\ supernatant}{Number\ of\ captured\ cells} \times 100\%$. Cell viability was detected by live/dead staining method. The released cells were added to the well plates and incubated in high sugar

DMEM for 6, 24 and 48 h, respectively. The supernatant was then removed and after washing with PBS buffer, Calcein-AM/PI double staining was used to evaluate the viability according to the instructions of manufacturer. Cells labeled with Calcein-AM only were counted as viable. In addition, the viability of released cells was evaluated by CCK-8 assay after incubation with high sugar DMEM for 6, 24 and 48 h. The released cells were incubated for 48 h and transferred to a new well plate for further incubation and passaged when the cells spread on the bottom of the plate.

1.10 Cancer cell release purity assay

WBCs and HeLa cells were mixed in PBS to prepare simulated blood samples, which were released by red light irradiation after co-incubation with g@SoS-PACF. Then the released cells were stained, and the number of released CTCs and WBCs was observed under a fluorescence microscope to calculate the release purity. The release purity was defined as the ratio of the number of released cancer cells to the total number of released cells.

1.11 Detection of CTCs from clinical blood samples

Peripheral blood samples from 15 tumor patients and 4 healthy volunteers were collected in anticoagulation tubes, treated with ACK lysis buffer within a short period of time, and incubated with g@SoS-PACF substrate for detection according to the above procedure. After washing, the cells were sequentially fixed with 2.5% glutaraldehyde for 1 h, permeabilized with 0.5% Triton X-100 solution for 10 min, and blocked with 1% BSA solution for 30 min and then stained with anti-CD45 (20 μg mL^{-1}) and PanCK (20 μg mL^{-1}) overnight at 4℃ in the dark. Finally, they were stained with DAPI (5 μg mL^{-1}) for 15 min and observed under a laser confocal microscope.

1.12 Ethical approval

All experiments were performed in accordance with the tenets of the Declaration of Helsinki, and approved by the Institutional Animal Care and Use Committee of Southwest Jiaotong University (No. SWJTU-2503-045). Informed consents were obtained from the human participants of this study.

2. Additional Scheme

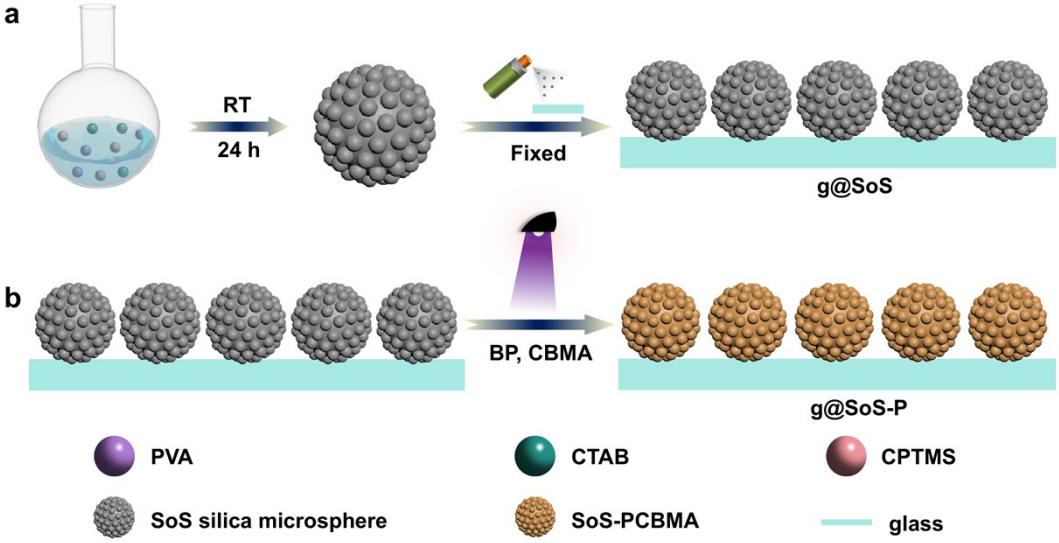

Scheme S1. Schematic illustration of the preparation process for g@SoS substrates (a) and g@SoS-P substrates (b).

2. Additional Figures

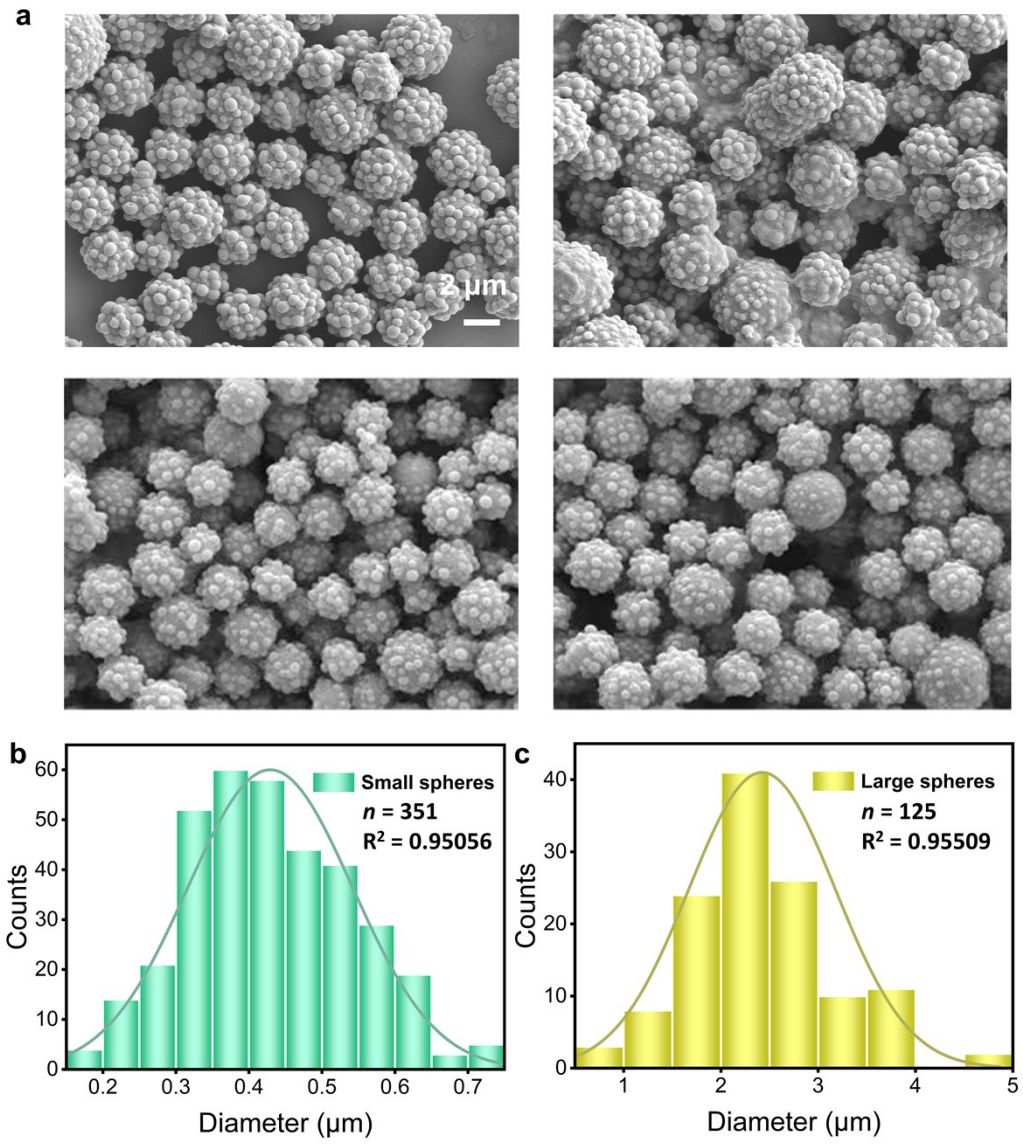

Figure S1. SEM images of SoS silica microspheres (a), and diameter distributions of small (b) and large (c) spheres on SoS silica microspheres. The particle size distributions were determined by measuring randomly selected microspheres/nanospheres from SEM images. The sample size (n) and coefficient of determination (R^2) for the Gaussian fitting are indicated in the corresponding panels: for small spheres, n = 351 and R^2 = 0.95056; for large spheres, n = 125 and R^2 = 0.95509.

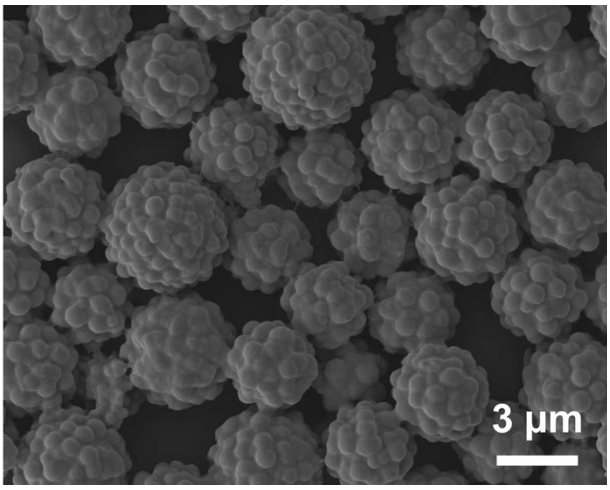

Figure S2. SEM image of the g@SoS-P substrate.

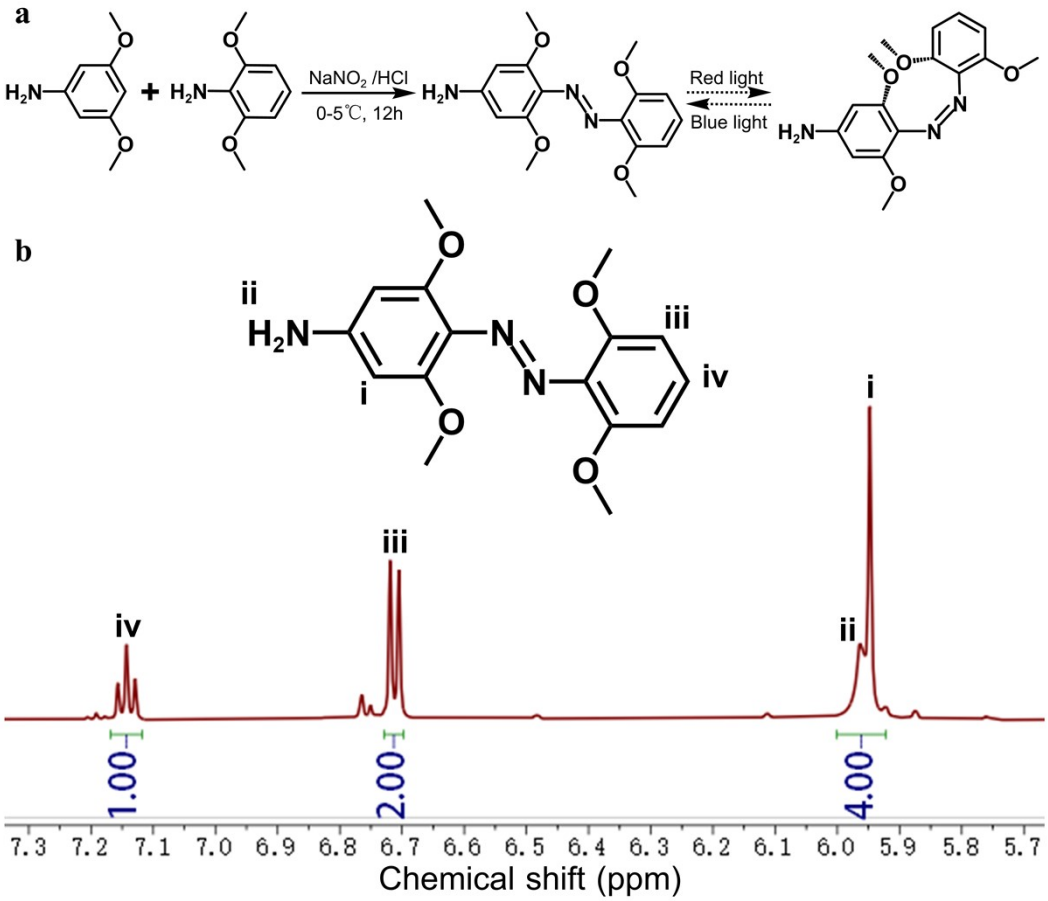

Figure S3. (a) The synthesis roadmap of mAzo. (b) 1H-NMR image of trans mAzo. The chemical shift at i corresponds to i: δ = 5.95 (s, 2H; Ar-H) in trans mAzo, the chemical shift at ii corresponds to ii: δ = 5.96 (s, 2H; Ar-NH_2); the chemical shift at iii corresponds to iii: δ = 6.73 (d, J = 8.4 Hz, 2H; Ar-H); the chemical shift at iv corresponds to iv: δ = 7.14 (t, J = 8.3 Hz, 1H; Ar-H), demonstrating the synthesis of trans mAzo.

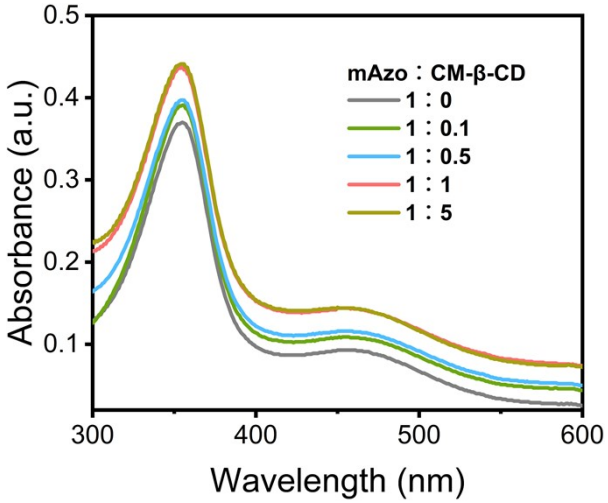

Figure S4. UV-vis absorption spectra of mAzo bound to CM-β-CD.

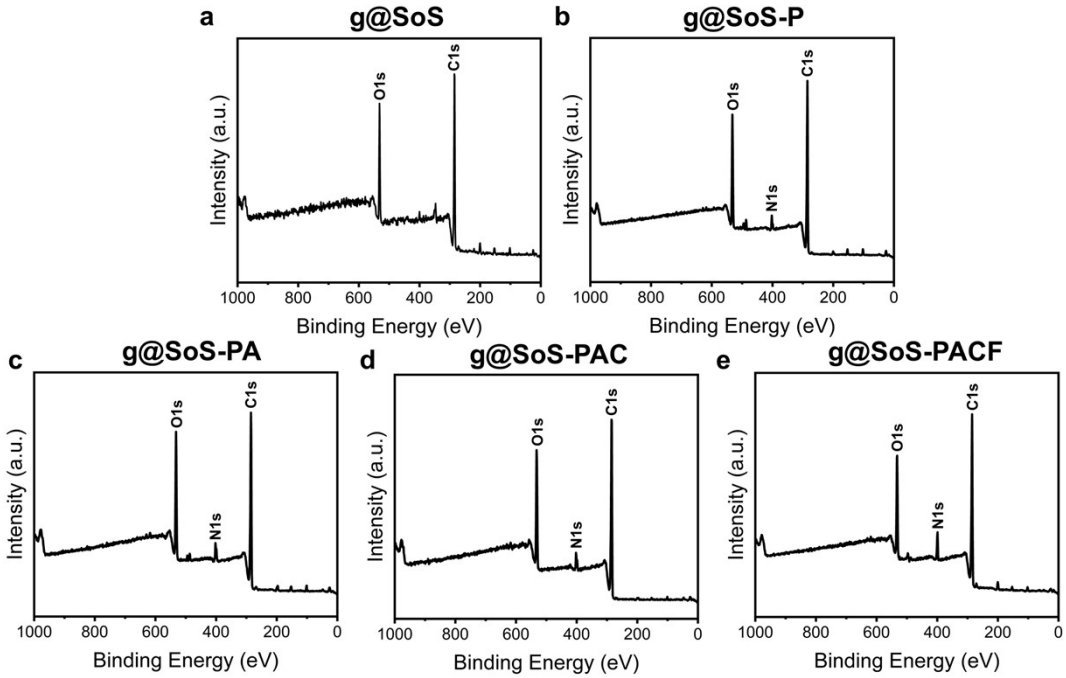

Figure S5. XPS spectra of the g@SoS (a), g@SoS-P(b), g@SoS-PA (c), g@SoS-PAC (d) and g@SoS-PACF (e) substrates.

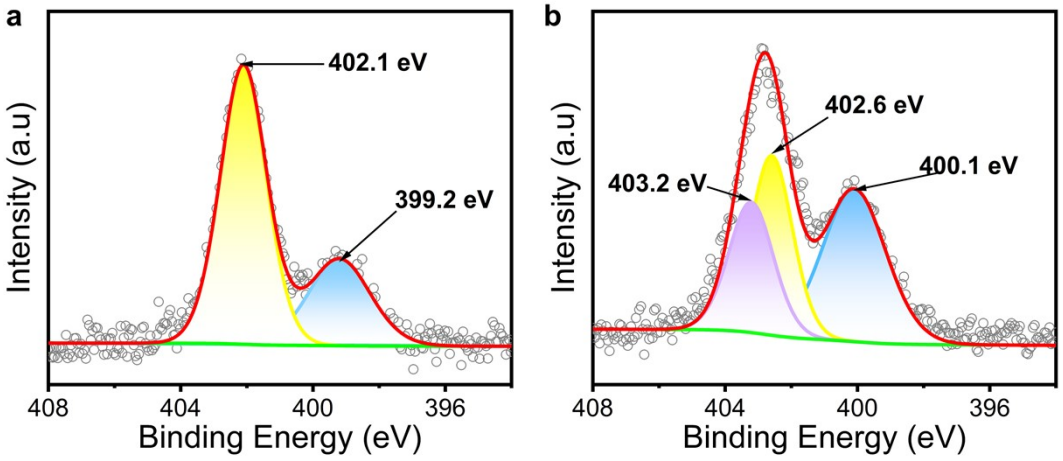

Figure S6. XPS high-resolution N 1s spectra of g@SoS-P (a) and g@SoS-PA (b) substrates.

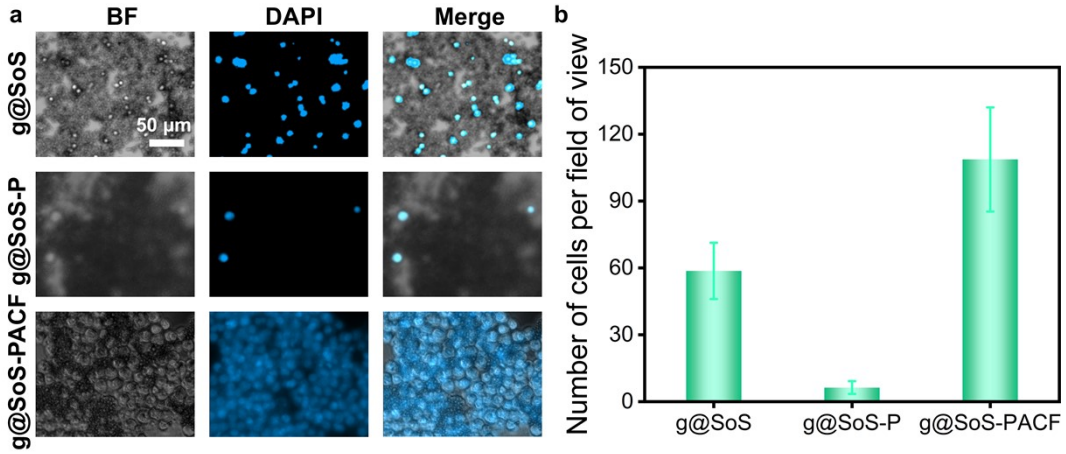

Figure S7. (a) Bright-field (BF) and fluorescence images and (b) corresponding quantification of HeLa cells captured by g@SoS, g@SoS-P, and g@SoS-PACF substrates.

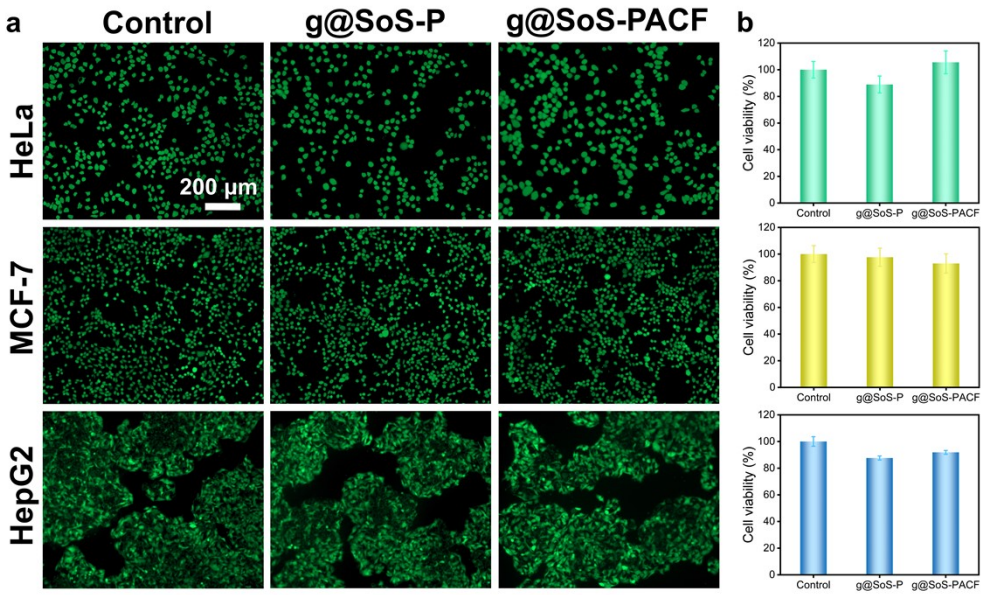

Figure S8. (a) The live/dead staining and (b) viability analysis of HeLa, MCF-7, and HepG2 cells following 24-hour incubation with different substrates.

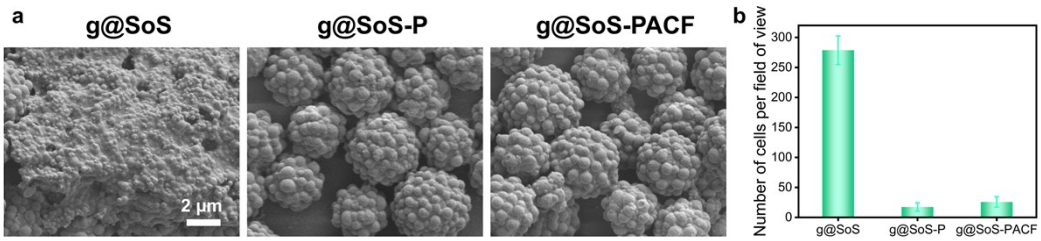

Figure S9. (a) SEM images and (b) corresponding quantitative analysis of platelet adhesion on g@SoS, g@SoS-P, and g@SoS-PACF substrates.

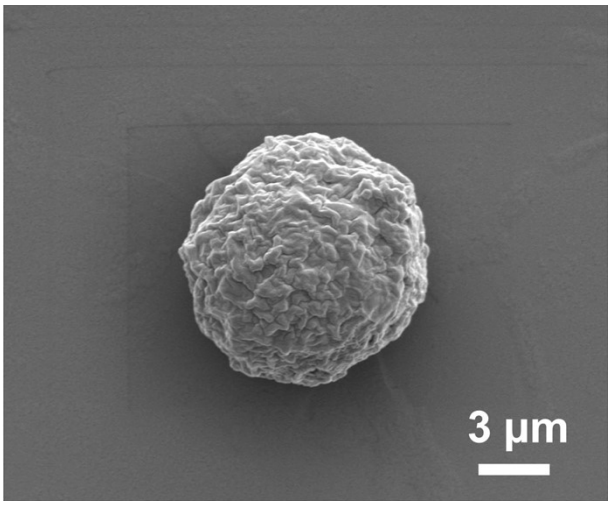

Figure S10. SEM image of released HeLa cells.

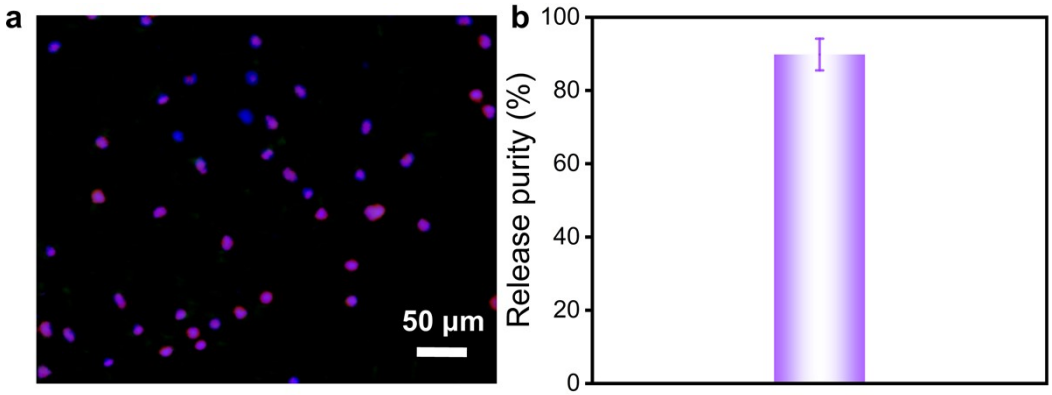

Figure S11. (a) Immunofluorescence image of released CTCs and WBCs, and (b) the corresponding CTC purity.

4. Additional Tables

Table S1. Atomic content of various substrates obtained by XPS analysis.

Sample	Compositions (at. %)		
	C (%)	O (%)	N (%)
g@SoS	72.5	17.8	3.8
g@SoS-P	72.3	20.4	4.4
g@SoS-PA	69.8	20.8	6.2
g@SoS-PAC	72.6	20.3	5.6
g@SoS-PACF	71.1	18.8	7.2

Table S2. Comparison of CTC Capture Methods

Platfrom	Capture Efficiency	Release Efficiency	Cell Viability	Ref.
MagSweeper	62%	N/A	51%	3
Engineered nanobioprobes	89%	65%	70%	4
The cellsearch system	85%	N/A	N/A	5
Immuno-magnetic separation technique	~90%	~86%	81%	6
Immuno-separation technique	87%	91%	86%	7
Microfluidic device	>65%	N/A	98.5%	8
Microfluidic device	50%	N/A	N/A	9
Microfluidic device	74%~94%	N/A	N/A	10
Microfluidic device	80%	N/A	N/A	11
3D micro/nanostructure microfluidic device	~84%	N/A	N/A	12
g@SoS-PACF	83.3%~92.7%	>94%	>89%	This work

Table S3. Basic information of cancer patients and healthy donors.

Diagnosis	Sample ID	Gender	Age	Clinical stage	Blood sample volume/mL	CTCs counts/mL
nasopharyngeal	1	male	58	IV	1	6
laryngeal	2	male	77	IV	1	16
lung	3	male	56	IV	1	11
oral	4	male	66	IV	1	5
gastric	5	female	78	IV	1	2
colon	6	male	59	III	1	13
intrahepatic cholangio	7	male	56	III	1	2
rectal	8	male	60	IV	1	4
oropharyngeal	9	male	76	IV	1	10
malignant pleural tumor	10	male	18	IV	1	7
esophageal	11	male	49	IV	1	4
cervical	12	female	58	III(figo)	1	2
rectal	13	male	70	III	1	14
liver neuroendocrine	14	male	70	IV	1	3
rectal	15	female	72	III	1	8
healthy donor	16	female	24	N/A	1	0
healthy donor	17	male	72	N/A	1	0
healthy donor	18	female	55	N/A	1	0
healthy donor	19	male	25	N/A	1	0

5. Additional References

1 D. Wang, M. Wagner, H.-J. Butt and S. Wu, *Soft Matter*, 2015, **11**, 7656–7662.

2 A. Adham, R. Harald, M. Peter and Z. Haifei, *Adv Mater*, 2012, **24**, 6042–6048.

3 A. H. Talasaz, A. A. Powell, D. E. Huber, J. G. Berbee, K.-H. Roh, W. Yu, W. Xiao, M. M. Davis, R. F. Pease, M. N. Mindrinos, S. S. Jeffrey and R. W. Davis, *PNAS*, 2009, **106**, 3970–3975.

4 M. Xie, N.-N. Lu, S.-B. Cheng, X.-Y. Wang, M. Wang, S. Guo, C.-Y. Wen, J. Hu, D.-W. Pang and W.-H. Huang, *Anal Chem*, 2014, **86**, 4618–4626.

5 W. J. Allard, J. Matera, M. C. Miller, M. Repollet, M. C. Connelly, C. Rao, A. G. Tibbe, J. W. Uhr and L. W. Terstappen, *Clin Cancer Res*, 2004, **10**, 6897–6904.

6 S. Guo, H. Huang, X. Deng, Y. Chen, Z. Jiang, M. Xie, S. Liu, W. Huang, X. Zhou, *Nano Res.*, 2018, **11**, 2592-2604.

7 Y. Xiao, L. Lin, M. Shen, X. Shi, *Bioconjugate chem.*, 2020, **31**, 130-138.

8 S. Nagrath, L. V. Sequist, S. Maheswaran, D. W. Bell, D. Irimia, L. Ulkus, M. R. Smith, E. L. Kwak, S. Digumarthy and A. Muzikansky, *Nature*, 2007, **450**, 1235–1239.

9 A. D. Hughes, J. Mattison, L. T. Western, J. D. Powderly, B. T. Greene and M. R. King, *Clin Chem*, 2012, **58**, 846–853.

10 Y. Zhou, Z. Dong, H. Andarge, W. Li and D. Pappas, *Analyst*, 2020, **145**, 257–267.

11 J. Yin, L. Mou, M. Yang, W. Zou, C. Du, W. Zhang and X. Jiang, *Anal Chim Acta*, 2019, **1060**, 133–141.

12 G. He, C. Yang, J. Feng, J. Wu, L. Zhou, R. Wen, S. Huang, Q. Wu, F. Liu, H. Chen, T. Hang, X. Xie, *Adv. Funct. Mater.*, 2019, **29**, 1806484.